J Neurophysiol 115: 3217–3228, 2016.
First published April 6, 2016; doi:10.1152/jn.01122.2015.

Development of a spontaneously active dorsal root ganglia assay using multiwell multielectrode arrays

Kim Newberry,[1] Shuya Wang,[1] Nina Hoque,[1] Laszlo Kiss,[2] Michael K. Ahlijanian,[1] James Herrington,[1] and John D. Graef[1]

[1]*Genetically Defined Diseases, Bristol-Myers Squibb Company, Wallingford, Connecticut; and* [2]*Leads Discovery and Optimization, Bristol-Myers Squibb Company, Wallingford, Connecticut*

Submitted 17 December 2015; accepted in final form 5 April 2016

Newberry K, Wang S, Hoque N, Kiss L, Ahlijanian MK, Herrington J, Graef JD. Development of a spontaneously active dorsal root ganglia assay using multiwell multielectrode arrays. *J Neurophysiol* 115: 3217–3228, 2016. First published April 6, 2016; doi:10.1152/jn.01122.2015.—In vitro phenotypic assays of sensory neuron activity are important tools for identifying potential analgesic compounds. These assays are typically characterized by hyperexcitable and/or abnormally, spontaneously active cells. Whereas manual electrophysiology experiments provide high-resolution biophysical data to characterize both in vitro models and potential therapeutic modalities (e.g., action potential characteristics, the role of specific ion channels, and receptors), these techniques are hampered by their low throughput. We have established a spontaneously active dorsal root ganglia (DRG) platform using multiwell multielectrode arrays (MEAs) that greatly increase the ability to evaluate the effects of multiple compounds and conditions on DRG excitability within the context of a cellular network. We show that spontaneous DRG firing can be attenuated with selective Na^+ and Ca^{2+} channel blockers, as well as enhanced with K^+ channel blockers. In addition, spontaneous activity can be augmented with both the transient receptor potential cation channel subfamily V member 1 agonist capsaicin and the peptide bradykinin and completely blocked with neurokinin receptor antagonists. Finally, we validated the use of this assay by demonstrating that commonly used neuropathic pain therapeutics suppress DRG spontaneous activity. Overall, we have optimized primary rat DRG cells on a multiwell MEA platform to generate and characterize spontaneously active cultures that have the potential to be used as an in vitro phenotypic assay to evaluate potential therapeutics in rodent models of pain.

DRG; MEA; nociceptors; sensory; spontaneous activity

NEW & NOTEWORTHY

This paper describes the development and use of an in vitro spontaneously active embryonic rat dorsal root ganglia (DRG) assay, as measured by multiwell multielectrode arrays. The authors have demonstrated that these cells can be cultured to promote high levels of intrinsic excitability that can be attenuated with clinically effective analgesics. With the development of a higher throughput, the functional DRG assay allows for identification and characterization of potential pain therapeutics in a manner conducive to translational drug discovery.

DORSAL ROOT GANGLIA (DRG) are clusters of neuronal sensory cell bodies located outside of the central nervous system along the spinal cord that conduct sensory signals originating from the periphery to the spinal cord. Under normal physiologic conditions, they exhibit limited spontaneous activity in vitro (Ma and LaMotte 2007; Xie et al. 2010) and in vivo (Djouhri et al. 2015; Weng 2012). However, following nerve injury or inflammation, DRG cells have been shown to become hyperexcitable (Djouhri et al. 2015; Study and Kral 1996; Weng 2012) and therefore, thought to play a major role in generating and maintaining chronic pain states (Djouhri et al. 2006; Xie et al. 2005).

The limited spontaneous activity under physiological conditions, together with the low throughput of manual electrophysiology recordings, has made it difficult to screen compounds for the ability to attenuate DRG hyperexcitability and by extension, potential efficacy in in vivo pain models. Multielectrode arrays (MEAs) are a useful tool for monitoring the functional activity of several individual, electrically excitable cells within a larger population. MEA platforms allow for the noninvasive, longitudinal monitoring of cellular networks over weeks and months to evaluate activity patterns during development, as well as any functional effects of acute and chronic treatment paradigms (Massobrio et al. 2015). Recently, the availability of multiwell MEA plates has allowed for increased throughput, offering the ability to perform complete concentration-effect curves of several compounds on cell populations that have been exposed to the same culture conditions (McConnell et al. 2012).

To date, only one attempt to establish an in vitro pain phenotype in either DRG or nociceptor neurons using MEAs has been reported (Wainger et al. 2015). Whereas these authors were able to demonstrate increased sensitization to capsaicin-induced activity in oxaliplatin-treated nociceptors, spontaneous DRG or nociceptor activity has yet to be demonstrated with MEA recordings in vitro. The establishment of a phenotypic DRG assay comprising substantive and persistent spontaneous activity would therefore provide a valuable in vitro model of hyperexcitability.

In this study, we demonstrate the optimization of primary rat DRG cells on a multiwell MEA platform to generate spontaneously active DRG cultures that can be used to assess both inhibitory and excitatory drug effects. This assay can be used to characterize activity patterns from hyperexcitable DRG populations with greater throughput than manual electrophysiology and single-well MEA platforms, making it useful for in vitro evaluations of a compound's potential efficacy in ameliorating pain-like states.

Address for reprint requests and other correspondence: J. D. Graef, Genetically Defined Diseases, Bristol-Myers Squibb, 5 Research Pkwy., Wallingford, CT 06492 (e-mail: john.graef@bms.com).

METHODS

Dissection. Sprague-Dawley rats (Charles River Laboratories, Wilmington, MA) were used in accordance with the guidelines of the Animal Care and Use Committee of Bristol-Myers Squibb and the guidelines published by the National Institutes of Health, "Guide for the Care and Use of Laboratory Animals," including measures to eliminate suffering and to reduce animal numbers to a minimum. Research protocols were approved by the Bristol-Myers Squibb Animal Care and Use Committee. Briefly, cells were prepared from embryonic day 15 pregnancy-staged rats (embryonic day 0 = first day following mating). Rats were euthanized with CO_2, the uterus was removed, and under a dissection microscope, embryos were removed and placed in a petri dish filled with HBSS, supplemented with HEPES (1%) and glucose (2%) on ice. With the use of microscissors, the head and posterior parts were cut away, and tissue on both sides of the spinal cord was removed. The meninges were removed, and individual ganglia were dissected from the entire length of the vertebral column and placed in ice-cold HBSS.

Cell isolation. All steps were performed under sterile conditions in a tissue-culture hood. Fresh medium and freshly thawed supplements and reagents were used. The dissociation and trituration steps were performed in Ca/Mg-free HBSS (Thermo Fisher Scientific Life Sciences, Waltham, MA). DRG cells were isolated using the Papain Dissociation System (Worthington Biochemical, Lakewood, NJ), following the manufacturer's instruction.

Multiwell MEA preparation. MEA plates were composed of 12 or 48 wells, with each well containing an array of 64 or 16 embedded gold electrodes, respectively (12-well: ~30 μm diameter, 200 μm center-to-center spacing; 48-well: ~40–50 μm diameter, 350 μm center-to-center spacing), with integrated ground electrodes, for a total of 768 channels (Cat. #M768-KAP; Axion BioSystems, Atlanta, GA). The day before dissection, MEA wells were coated with a 50-μg/ml solution of poly-D-lysine (Sigma, St. Louis, MO) for 2 h in a 37°C cell-culture incubator. Plates were rinsed with sterile, deionized water four times and air dried in a biological safety cabinet overnight.

Cell plating. DRG cells were cultured in medium containing the following: Neurobasal medium L-glutamine (Thermo Fisher Scientific Life Sciences), supplemented with GlutaMAX (1%; Thermo Fisher Scientific Life Sciences), PenStrep (1%; Thermo Fisher Scientific Life Sciences), B27 (2%; Thermo Fisher Scientific Life Sciences), NaCl (5 mg/ml; Sigma), nerve growth factor (NGF) 2.5S (100 ng/ml; BD Biosciences, San Jose, CA), uridine (17.5 μg/ml; Amresco, Solon, OH), and 5-fluoro-2′-deoxyuridine (7.5 μg/ml; Sigma). On the day of culture, laminin (Sigma) was prepared in cell-culture medium without antimitotics (20 μg/ml), and with the use of the dotting method, recommended by Axion BioSystems, a 5-μl droplet was placed in the center of each well over the MEA electrodes. The plates were incubated for 1 h at 37°C, after which the laminin was removed, leaving only a coating in the wells. Before the laminin was allowed to dry, a 5-μl drop of media containing DRG cells was placed over the laminin coating. The cells were allowed to attach to the substrate in a cell-culture incubator for 1 h, and then 750 μl culture medium was added to the wells. Cells were grown at 37°C in a humidified 5% CO_2/95% O_2 incubator. To maintain the culture, a 50% medium change with fresh 37°C culture medium was performed every 3–4 days.

Compound addition. Compounds were dissolved in either DMSO or sterile, distilled water as a 10-mM stock and then diluted further in their respective solvents or in water, if soluble, to reach a 100× stock concentration. Compounds were then diluted 1:100 directly into the culture (7.5 μl in 750 μl culture medium volume). Of note, there was an acute effect of DMSO when final concentrations as low as 0.13% were introduced into the culture, showing a significant increase in DRG spontaneous activity (baseline: 10.07 ± 2.449 spikes/min; 0.13% DMSO: 47.32 ± 13.92 spikes/min, $n = 6$). This effect lasted up to 30 min, after which, the spontaneous activity levels returned to baseline. This increase was not observed when a similar volume of water was introduced into the cultures. Additionally, serial additions of 0.13% DMSO were added up to five times in the same well for a cumulative concentration of 0.65%, with all DMSO-induced increases in activity returning to baseline levels within the 30-min interval after each DMSO addition. This allowed for the possibility of five-point concentration response curves within each well.

Data acquisition. Spontaneous network activity from DRG cultures grown on MEA plates was recorded using hardware and software from Axion BioSystems. The hardware consisted of the Maestro 768 channel amplifier, Middle-man data acquisition interface, and a personal computer. Data were acquired using Axion BioSystems' Integrated Studio (AxIS) software. Channels were sampled simultaneously with a gain of 1,200× and a sampling rate of 12.5 kHz/channel. All recordings were conducted at 37°C [with the exception of 1 of the experiments (see Fig. 2*A*), which was recorded at 42°C]. Plates containing the cultures were placed into the Maestro, and spontaneous activity of each well was recorded. For recordings, a Butterworth band-pass filter (with a high-pass cutoff of 200 Hz and a low-pass cutoff of 3,000 Hz) was applied, along with a variable threshold spike detector set at 6 SD of the root mean squared of the noise on each channel. Recordings (~5 min) were taken, and data were saved to two different file types simultaneously: a raw data file (*.raw file) that included all recorded data and an AxIS Spike file (*.spk file) that includes time stamps and waveforms for all detected spikes.

Data analysis. Time-stamp and waveform data for all spikes were processed through a custom-analysis program written in MATLAB (MathWorks, Natick, MA; Fig. 1*A*) to sort all spikes into their respective wells and to calculate well-wide averages for various spike and burst metrics. Spikes from each electrode were first sorted based on amplitude by fitting a spike-amplitude histogram with a probability distribution curve using the MATLAB function fitdist. The MATLAB function findpeaks was then used to group binned spikes according to the number of peaks. An example trace and fitted histogram showing two groups of recorded spikes with different amplitudes are shown in Fig. 1, *B* and *C*. All electrodes with recorded activity of five spikes/min or greater were considered active and included in the analysis. Following the spike-sorting process, some electrodes had up to three separate active units. On average, each well had approximately eight active units (Table 1). Individual bursts were detected using a rank surprise method [see Gourevitch and Eggermont (2007) for explanation and MATLAB code]. Functional connections between individual units were determined by a statistically significant correlation coefficient generated by the MATLAB function corrcoef ($P < 0.01$). A flow chart summarizing the overall analysis is shown in Fig. 1*D*.

All data reflect well-wide averages, with reported n representing the number of wells per condition. Data were exported to an Excel worksheet and then imported into Spotfire (Tibco Software, Palo Alto, CA) for visualization and GraphPad Prism (GraphPad Software, La Jolla, CA) for analysis. Normalized data were determined by normalizing to within-well baseline or pretreatment conditions and then normalizing to the mean of all vehicle-treated control wells. This type of analysis was able to control for any nontreatment changes in DRG spontaneous activity through the experiment. All statistics are reported as ±SE.

Substance P ELISA. The concentration of substance P was measured using a commercially available substance P ELISA kit, as per the manufacturer's protocol (#KA0302; Thermo Fisher Scientific Life Sciences). Briefly, DRG cells were plated and cultured on 96-well plates under the same conditions used for plating and culturing on multiwell MEA plates. After 2 wk in culture [14 days in vitro (DIV)], cells were treated with compound, and then all media were removed 5 min post-treatment. The intracellular contents of the adherent cells were then extracted using radioimmunoprecipitation assay lysis buffer, according to the manufacturer's protocol (Sigma).

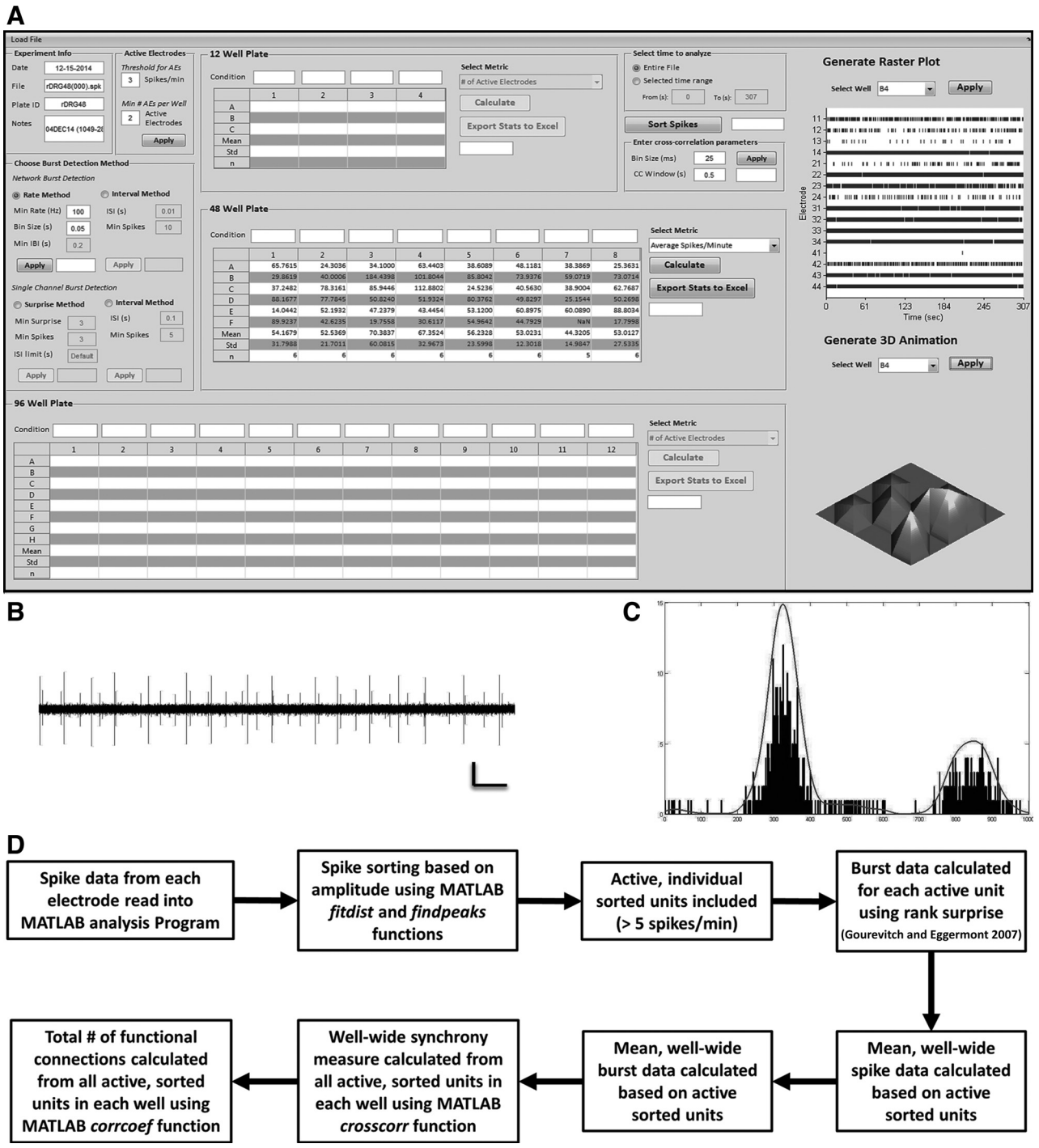

Fig. 1. Analysis of spontaneous DRG activity using MATLAB. *A*: custom graphical user interface (GUI) for analyzing and visualizing Axion BioSystems' MEA data. *B*: example trace recorded from an individual electrode showing extracellular potentials (spikes) from 2 putatively different DRG cells. *C*: spike-amplitude histogram generated in MATLAB for recorded electrode shown in *B*, with a fitted probability distribution curve (black line). *D*: flow chart summarizing the overall analysis in MATLAB.

RESULTS

Culture optimization. To create a higher throughput functional DRG assay in vitro, we attempted to optimize the overall activity using multiwell MEA plates. Early attempts displayed negligible, spontaneous DRG activity at various plating densities (50,000, 100,000, 150,000, and 200,000) using a standard Neurobasal culture medium. Although no spontaneous activity could be seen, transitory activity could be evoked in these cultures after the addition of 1 μM capsaicin or 200 μM menthol (data not shown).

To facilitate spontaneous DRG activity, we supplemented the culture media with 100 ng/ml NGF. Chronic NGF treatments have been shown to produce hyperexcitable adult DRG neurons in vitro (Kayano et al. 2013; Kitamura et al. 2005; Zhu et al. 2004) and to increase substance P release significantly in rat embryonic DRG cultures (Yang et al. 2007). The supple-

Table 1. *DRG 14 DIV functional metrics*

Spike Metrics	Value ± SE (*n*)	Burst Metrics	Value ± SE (*n*)
# of Active electrodes, out of 16	8.50 ± 0.57 (46)	Bursts/min	2.97 ± 0.32 (44)
Spike rate, Hz	1.14 ± 0.12 (46)	Burst length, s	1.09 ± 0.12 (44)
Spike amplitude, μV	27.95 ± 0.92 (46)	Interburst interval, s	8.85 ± 0.67 (44)
Spike duration, ms	1.20 ± 0.01 (46)	# of Spikes/burst	5.37 ± 0.12 (44)
Interspike interval, s	0.86 ± 0.03 (46)	Spike frequency in burst, Hz	21.08 ± 3.16 (44)
Interspike interval CV	0.91 ± 0.05 (46)	% of Total spikes within a burst	23.18 ± 0.45 (44)
Crosscorrelation probability	0.011 ± 0.001 (46)		
# of Functional connections/well	2.00 ± 0.26 (25)		

CV, coefficient of variation.

mentation with NGF, along with the addition of the antimitotic agents uridine and 5-fluoro-2′-deoxyuridine to the culture medium, 24 h after seeding, led to a noticeable increase in the number of spontaneously active electrodes in each well. The addition of uridine and 5-fluoro-2′-deoxyuridine is needed if culturing beyond 4 DIV to prevent Schwann cell proliferation and DRG detachment from the substrate (Liu et al. 2013). Finally, by increasing the NaCl concentration in the Neurobasal medium from 50 mM to a more physiologically relevant concentration of 140 mM, we were able to produce significantly increased levels of spontaneous DRG firing within the majority of wells. This increase in activity is illustrated in Fig. 2. At 7 DIV, DRG cultures grown in 140 mM NaCl exhibited a nearly threefold increase in the rate of spontaneous activity compared with DRG cells cultured in 50 mM NaCl (Fig. 2*A*; 50 mM NaCl: 12.8 ± 4.6 spikes/min, $n = 4$ wells; 140 mM NaCl: 34.9 ± 8.2 spikes/min, $n = 4$ wells; $P < 0.05$ unpaired *t*-test). In addition, higher rates of DRG activity could be evoked by increasing the temperature of the cultures (Fig. 2*A*; 50 mM NaCl at 37°C: 34.9 ± 8.2 spikes/min, $n = 4$ wells; 140 mM NaCl at 42°C: 58.4 ± 11.7 spikes/min, $n = 4$ wells; $P < 0.05$, paired *t*-test) or with the addition of the transient receptor potential cation channel subfamily V member 1 agonist capsaicin (Fig. 2*B*; 2.3 ± 0.4-fold increase at 1 μM, $n = 8$). These culture conditions therefore provided increased levels of spontaneous activity, resulting in the ability to assess both inhibitory and excitatory pharmacological treatments.

After establishing the preferred culture conditions that included 100 ng/ml NGF and 140 mM NaCl, we next assessed the effects of cell density on spontaneous DRG activity. As can be seen in Fig. 3, the higher densities of DRG cells plated onto the MEA resulted in higher rates of activity (Fig. 3*B*). The rate of spontaneous DRG activity was also dependent on the time in culture, with lower levels of activity recorded after 5 days in culture, followed by a steady increase in firing rates up to 2 wk after plating. This time-dependent increase in activity was not seen with higher plating densities (100,000 cells/well) that exhibited higher initial activity rates that remained stable or decreased over time. Figure 3*A* shows a representative screen shot of real-time, spontaneous activity recorded with Axion BioSystems' acquisition software AxIS. A heat map depicting spontaneous firing rates for each electrode in each of the 12 wells is shown with DRG densities of 25,000, 50,000, and 75,000 cells/well plated in a 12-well MEA plate. In addition, a representative image is shown depicting the distribution and morphology of DRG neurons plated on an MEA at a density of 50,000 cells/well after 11 days in culture. Groups of DRG cells and processes can be seen surrounding the electrodes.

For all subsequent experiments, a plating density of 50,000 cells/well was used, along with culture media, supplemented with 100 ng/ml NGF and 140 mM NaCl. Peak activity levels occurred between 11 and 14 DIV. The firing, network, and burst properties of these cultures at 14 DIV are shown in Table 1. On average, approximately one-half (8.5 ± 0.6) of all available electrodes per MEA was active, with an average firing rate of 1.14 ± 0.12 Hz. A majority of the spontaneous activity was in the form of tonic firing. A relatively low burst rate was observed (2.97 ± 0.32 bursts/min), with 23.18 ± 0.45% of total recorded spikes occurring within a burst. Additionally, whereas DRG processes are evident during the second week of culture, very few of the spontaneously active cells formed functional connections, as defined by statistically

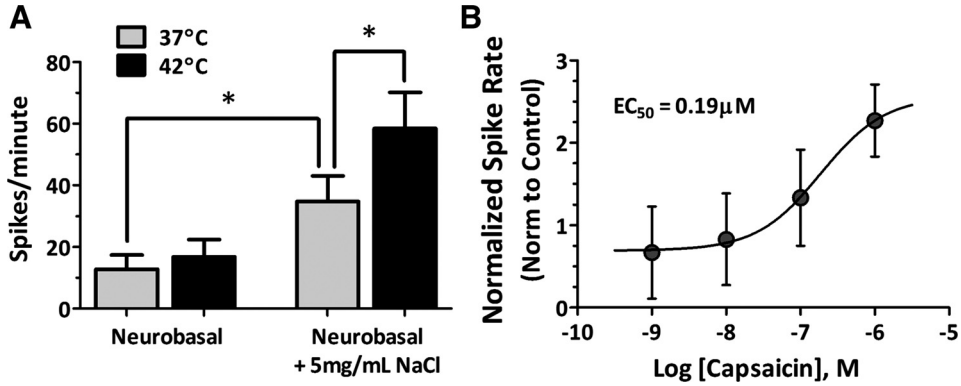

Fig. 2. NaCl, heat, and capsaicin increase spontaneous DRG activity. *A*: a significant increase in spikes per minute in response to higher concentrations of NaCl in the culture medium is shown in the light gray bars (*$P < 0.05$, unpaired *t*-test). Heat application (42°C; dark gray bars) significantly increases the amount of spikes per minute only in DRG cultures exposed to higher concentrations of NaCl (*$P < 0.05$, paired *t*-test). *B*: concentration response curve for capsaicin-induced increases in activity. Spike rate is normalized to the average spontaneous spike rate of untreated control wells.

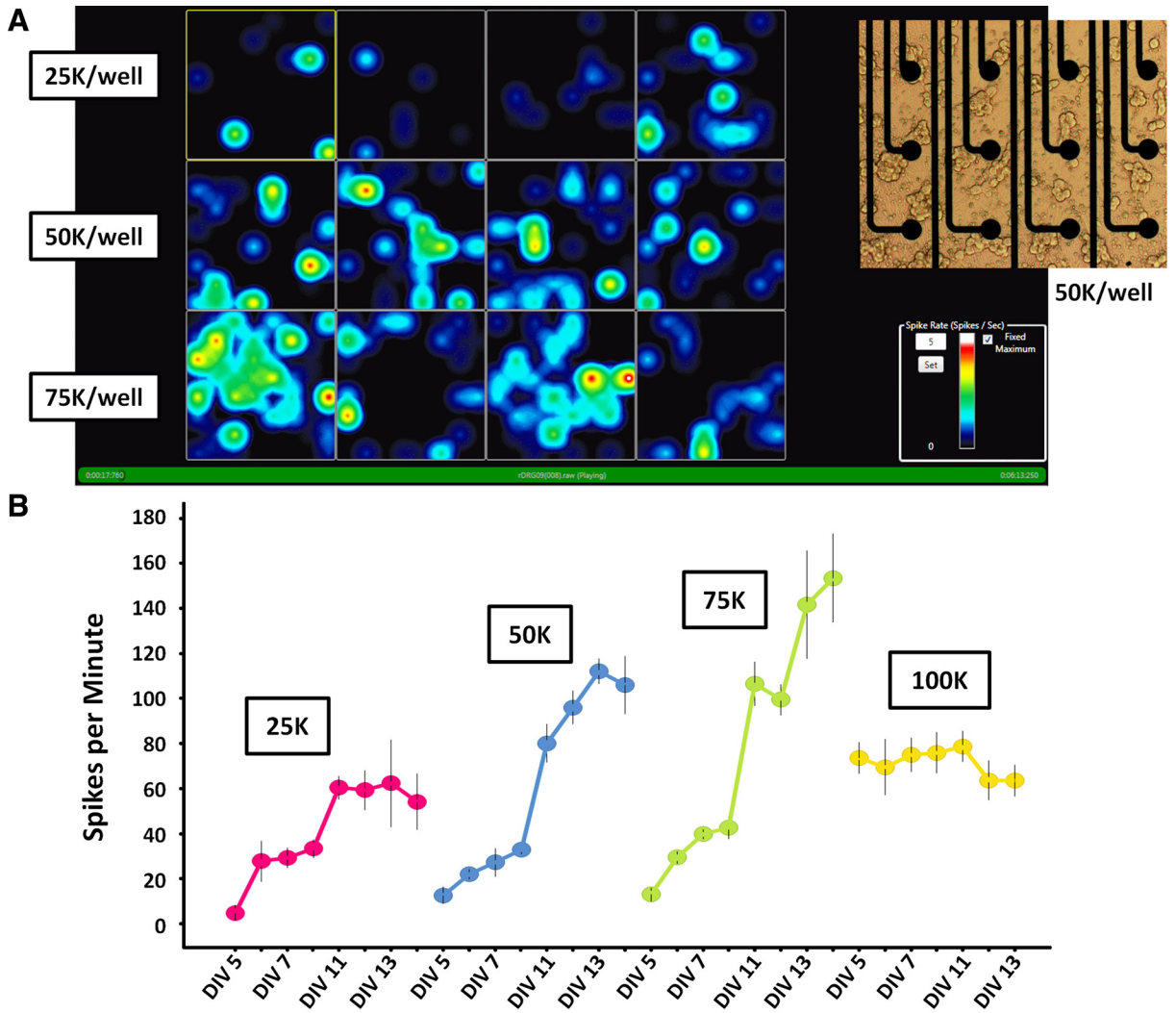

Fig. 3. Density-dependent increases in overall spontaneous activity. *A*: image of real-time firing rate heat map generated by AxIS software showing greater well-wide DRG activity as the density of plated cells over the MEA grid is increased. *Inset*: image of DRG cells and electrodes (black circles) on an MEA plated at 50,000 cells/well. *B*: spontaneous DRG activity plotted as spikes per minute over the first 2 wk in culture.

significant correlated activity. This is in contrast to hippocampal and cortical neurons, which tend to exhibit synchronous bursting patterns as a result of the presence of functional synapses (Chiappalone et al. 2007). Approximately one-half of the wells (25 out of 46) exhibited at least one functional connection, with an average of 2.00 ± 0.26 connections per MEA (Table 1).

As a proof-of-concept experiment, we attempted to culture adult mouse DRG cells on our multiwell MEA plates under the same conditions used for our embryonic rat DRG preparations. These adult DRG cells were significantly less active than embryonic rat DRG cells (0.41 ± 0.12 Hz) and exhibited a lower burst rate (1.03 ± 0.28 bursts/min). However, individual spike characteristics were similar (mean spike amplitude: 24.6 ± 1.5 μV; mean spike duration: 1.27 ± 0.06). These data indicate that recording spontaneous activity from adult rodent DRG cells is possible and that further optimization is necessary to produce cultures with activity levels similar to the embryonic rat DRG cultures described here.

Culture characterization. Once the DRG cell cultures were optimized for spontaneous activity, the identity of the ion channels and receptor systems that were either contributing to this activity or could be targeted to evoke further DRG excitability was determined. DRG neurons have been shown to have both TTX-sensitive (TTX-S) and TTX-resistant (TTX-R) Na^+ channels. Therefore, the effects of TTX on spontaneous DRG activity on our MEA system were examined. At both 7 and 14 DIV, TTX was able to abolish spontaneous activity fully at 1 μM (Fig. 4*A*); however, the potency of TTX was lower at 7 DIV (IC_{50} = 0.072 μM) compared with 14 DIV (IC_{50} = 0.011 μM). To validate the inhibitory effects of TTX on spontaneous activity, we performed whole-cell current-clamp recordings from a DRG neuron near an active electrode from a 12-well MEA plate. As can be seen in Fig. 4*B*, we were able to record spontaneous action potentials from this cell that could be blocked with 1 μM TTX (13 DIV, capacitance: 19.8 pF). To identify further which voltage-gated Na^+ channel (Na_V) subtypes contribute to this spontaneous activity, we used Protoxin II (ProTx-II), a tarantula peptide toxin selective for the TTX-S $Na_V1.7$ channel at low nanomolar concentrations (Schmalhofer et al. 2008). At 10 nM, a concentration reported to be selective for $Na_V1.7$, ProTx-II was much more potent at inhibiting

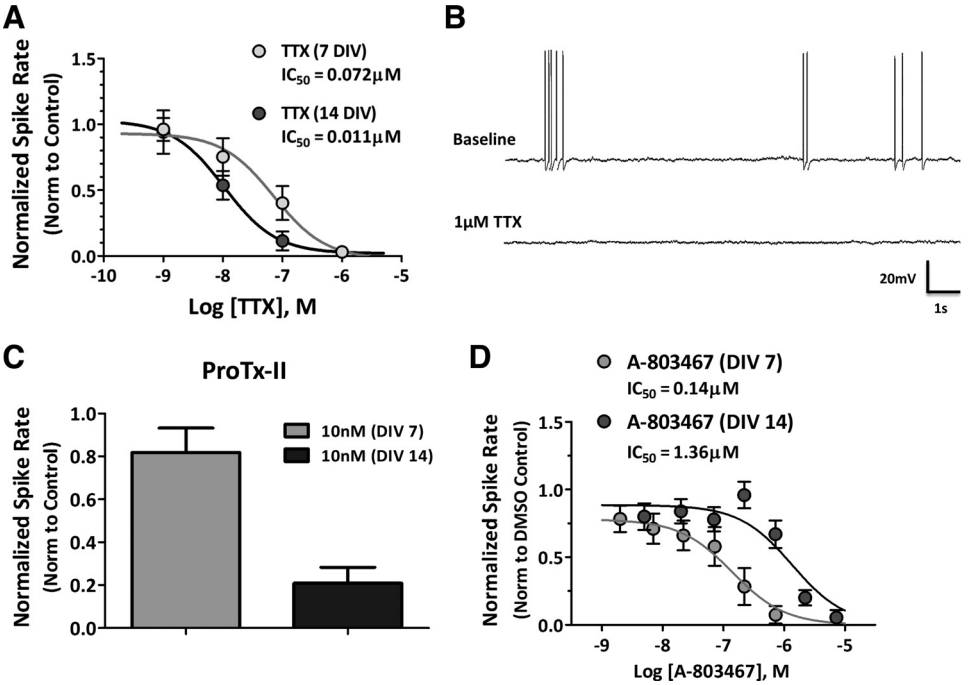

Fig. 4. Na_V channels contribute to spontaneous DRG activity. *A*: concentration response curves for TTX on spontaneously active DRG cultures at 7 DIV (light gray circles) and 14 DIV (dark gray circles). IC_{50} values are shown on the graph. *B*: whole-cell current-clamp recording of spontaneous action potentials from a DRG cell cultured on an MEA grid at 14 DIV (*top* trace) that have been abolished following application of 1 μM TTX (*bottom* trace). *C*: effect of 10 nM ProTx-II on spontaneously active DRG cultures at 7 DIV (light gray bar) and 14 DIV (dark gray bar). *D*: concentration response curves for A-803467 on spontaneously active DRG cultures at 7 DIV (light gray circles) and 14 DIV (dark gray circles). IC_{50} values are shown on the graph.

spontaneous DRG activity at 14 DIV compared with 7 DIV (Fig. 4*C*; 7 DIV: 18 ± 11% inhibition, $n = 6$; 14 DIV: 79 ± 7%, $n = 4$). In addition, A-803467, a selective inhibitor of the TTX-R $Na_V1.8$ channel (Jarvis et al. 2007), was able to block spontaneous DRG activity at both 7 and 14 DIV; however, the potency was 10-fold greater at 7 vs. 14 DIV (Fig. 4*D*). Taken together, these data indicate that both TTX-S and TTX-R channels contribute to the spontaneous firing of DRG cells recorded on our MEAs in a DIV-dependent manner. TTX-R Na_V channels predominate at 7 DIV, whereas TTX-S Na_V channels predominate as the cultures mature. Further validation of Na^+ channel involvement in DRG excitability is illustrated in Table 2 by the inhibitory effect of two other general Na^+ channel blockers, lidocaine and mexiletine.

Voltage-gated Ca^{2+} channels (Ca_V) play an important role in DRG excitability and neurotransmitter release and therefore, are key regulators of both normal and pain-related signaling (Zamponi et al. 2009). Therefore, we next investigated the effects of Ca_V channel inhibitors on DRG activity to determine the contribution to spontaneous firing (Table 2). Both N- and L-type Ca_V channels have been reported to play a role in mediating neurotransmitter release from rat sensory neurons (Heinke et al. 2004; Perney et al. 1986). As can be seen in Fig. 5*A*, nifedipine, an L-type Ca_V channel blocker, was able to inhibit spontaneous DRG activity at 10 μM (67.1 ± 10.5% inhibition of control, $n = 7$) but had no effect at 3 μM (117.2 ± 26.5% of control, $n = 6$). Additionally, ω-conotoxin MVIIA, an N-type Ca^{2+} channel blocker that has been demonstrated to be effective in models of chronic pain (Hama and Sagen 2009), had no effect on spontaneous activity at concentrations up to 1 μM and produced modest inhibition at 3 μM (74.4 ± 16.4% of control, $n = 8$; Fig. 5*A*). Similarly, SNX-482, a tarantula toxin and selective inhibitor of R-type Ca_V channel (Newcomb et al. 1998), also failed to attenuate spontaneous firing in our DRG cultures at concentrations up to 1 μM (Fig. 5*A*). In contrast to the high-threshold L-, N-, and R-type Ca_V channels that mediate neurotransmitter release, low-threshold (T-type) Ca_V channels are important regulators of DRG intrinsic excitability (Zamponi et al. 2009) and have also been implicated in pain transmission (Jevtovic-Todorovic and Todorovic 2006; Todorovic and Jevtovic-Todorovic 2006). Mibefradil, a selective T-type Ca_V channel at low micromolar concentrations (Clozel et al. 1997), demonstrated near-complete inhibition of DRG spontaneous activity at 10 μM. Whereas mibefradil has been shown to block L-type Ca_V channel as well at high concentrations (Bezprozvanny and Tsien 1995; Mishra and Hermsmeyer 1994), the concentration-response curve for mibefradil in Fig. 5*B* demonstrates an IC_{50} of 1.16 μM—a value similar to a previously reported IC_{50} of ~3 μM on rat DRG T-type Ca^{2+} currents (Todorovic and Lingle 1998)—thus indicating a prominent role for T-type Ca_V channels in spontaneous DRG activity. NiCl, another selective T-type Ca_V channel inhibitor (Lee

Table 2. *DRG ion channel pharmacology*

Compound (Na_V channels)	Effect at 14 DIV
TTX	IC_{50} = 0.011 μM (0.072 μM at 7 DIV)
Lidocaine	IC_{50} = 48 μM
Mexiletine	IC_{50} = 0.52 μM
Protoxin II	IC_{50} = 0.007 μM
A-803467	IC_{50} = 1.4 μM (0.14 μM at 7 DIV)
Compound (Ca_V channels)	
Nifedipine	67% Inhibition of activity at 10 μM
Conotoxin MVIIA	26% Inhibition of activity at 3 μM
SNX-482	No effect ≤1 μM
NiCl	34% Reduction in bursts at 100 μM
Mibefradil	IC_{50} = 1.16 μM
Compound (K_V channels)	
Linopirdine	EC_{50} = 0.4 μM
4-AP	Increased spontaneous activity at 3 and 10 μM
Retigabine	IC_{50} = 0.43 μM
Compound (Other)	
Capsaicin	EC_{50} = 0.19 μM

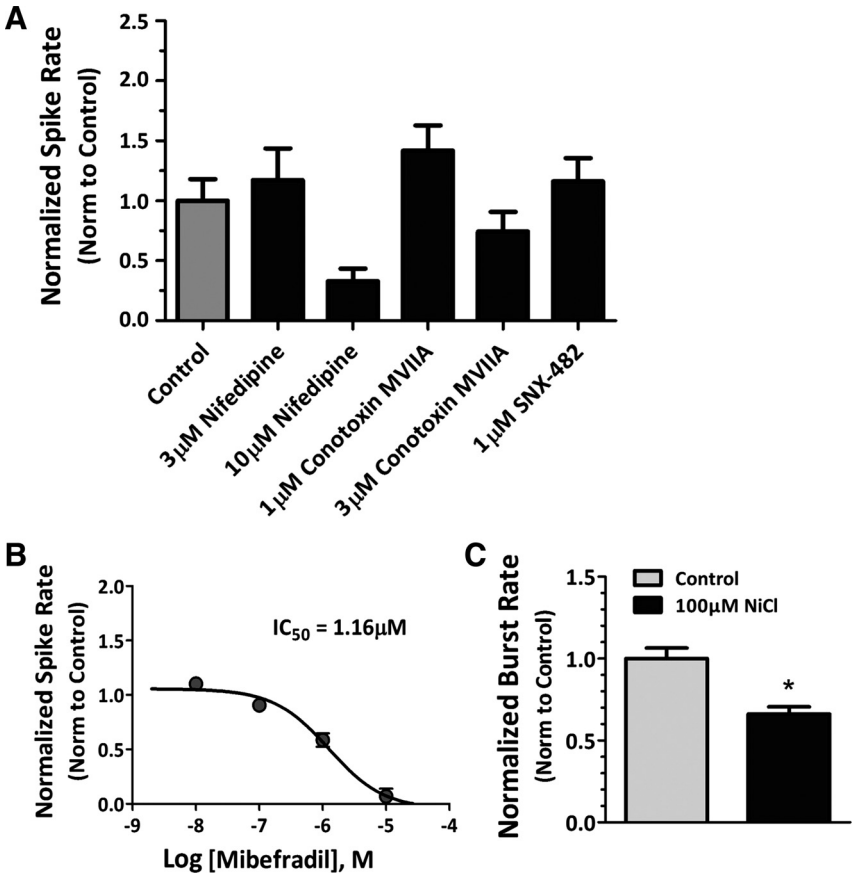

Fig. 5. T-Type Ca^{2+} channels contribute to spontaneous DRG activity. *A*: effect of varying concentrations of high-threshold Ca^{2+} channel blockers (dark gray bars) on spontaneously active DRG cultures 14 DIV compared with control wells (light gray bar). *B*: concentration response curve for mibefradil on spontaneously active DRG cultures at 14 DIV. IC_{50} value is shown on the graph. *C*: effect of 100 μM NiCl (dark gray bar) on spontaneously active DRG cultures at 14 DIV compared with control wells (light gray bar; $^*P < 0.05$, Mann-Whitney test).

et al. 1999), significantly decreased spontaneous bursts within the DRG culture at a concentration of 100 μM (66.2 $\pm$ 4.4% of control, $n = 3$; $P < 0.05$, Mann-Whitney test; Fig. 5*C*). This inhibition of bursting activity agrees with a previous study showing a suppression of action potentials in DRG neurons by Ni^{2+} (Abdulla and Smith 1997) and is in line with the reported role of T-type Ca_V channels in generating bursts of action potentials (Huguenard 1996). Since NiCl has been shown to be selective for the $Ca_V3.2$ T-type isoform over $Ca_V3.1$ and $Ca_V3.3$ (Lee et al. 1999), these data suggest that $Ca_V3.2$ may play a more prominent role in spontaneous DRG burst firing, whereas the other T-type isoforms contribute more to tonic DRG activity. However, further studies are needed to confirm this hypothesis. Overall, these findings indicate that T-type Ca^{2+} channels are the primary Ca_V channels contributing spontaneous rat DRG activity in our embryonic cultures.

Voltage-gated K^+ channels (K_v) are also expressed in DRG, and previous studies have demonstrated that K_v currents are reduced following nerve injury, resulting in hyperexcitability and hyperalgesia (Everill and Kocsis 2000). K_v channel subfamily KQT member 4 subunits are expressed in DRG, and the underlying M-current that these channels conduct is known to regulate excitability in a variety of central and peripheral neurons (Passmore et al. 2003). For this reason, we tested the M-channel blocker linopirdine and the K_v7 channel activator retigabine for effects on DRG spontaneous activity. The blocking of M-channels with linopirdine significantly enhanced DRG spontaneous firing (6.4 $\pm$ 1.1-fold over control at 10 μM) with an EC_{50} of 0.4 μM (Table 2). Conversely, the activation of K_v7 channels with retigabine abolished activity with an IC_{50} of 0.43 μM (Table 2). The relatively nonselective K_v inhibitor 4-aminopyridine was also tested, resulting in modest increases in spontaneous activity at both 3 μM (2.0 $\pm$ 0.3-fold over control, $n = 2$) and 10 μM (2.5 $\pm$ 0.2-fold over control, $n = 2$) concentrations (Table 2). These results demonstrate the functional presence of K^+ channels in our rat embryonic DRG cultures and their role in spontaneous activity.

In addition to probing ion channels, identification of the neurotransmitter systems involved in generating spontaneous DRG firing was examined. As can be seen in Fig. 6*A*, application of the major inhibitory and excitatory neurotransmitters GABA, glutamate, and *N*-methyl-D-aspartate (NMDA) had little, if any, effect on baseline activity rates. Correspondingly, picrotoxin ($GABA_A$ antagonist), 2,3-dihydroxy-6-nitro-7-sulfamoyl-benzo[f]quinoxaline-2,3-dione (NBQX; AMPA antagonist), and (2*R*)-amino-5-phosphonovaleric acid (APV; NMDA antagonist) also did not significantly alter baseline firing rates, indicating that these neurotransmitter systems do not contribute significantly to the spontaneous activity recorded in these DRG cultures (Fig. 6*B* and Table 3). We also investigated the role of L-732,138 [a highly potent and selective neurokinin 1 (NK1) receptor antagonist] and GR 159,897 (a selective NK2 receptor antagonist) in driving DRG spontaneous activity. Both 10 μM L-732,138 and 10 μM GR 159,897 completely abolish DRG spontaneous activity (Fig. 6). Further investigation demonstrated that GR 159,897 was much more potent at inhibiting activity, with an IC_{50} of 0.18 μM compared with L-732,138, which had an IC_{50} of 1.5 μM. Whereas L-732,138 has been shown to be a potent and selective inhibitor of the human NK1 receptor, it has been demonstrated to be

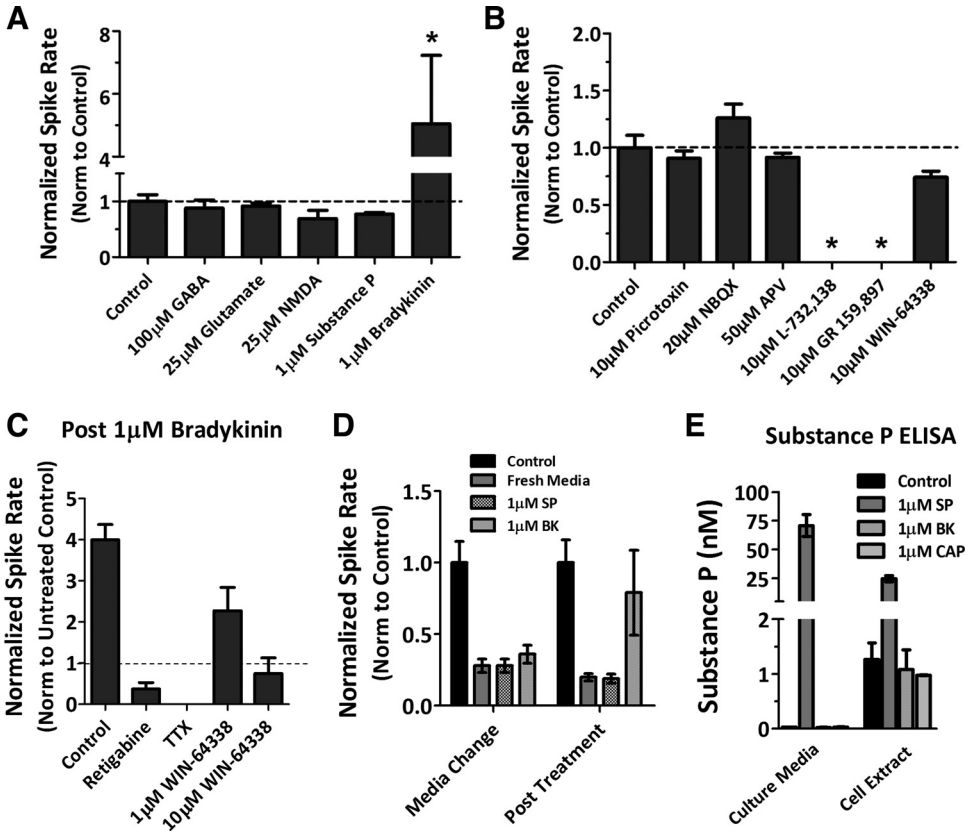

Fig. 6. Profile of ligand-gated receptors contributing to spontaneous DRG activity. *A*: effect of varying concentrations of neurotransmitters and peptides on spontaneously active DRG cultures at 14 DIV. Only bradykinin was able to alter spontaneous activity levels significantly (*$P < 0.05$, one-way ANOVA with Bonferroni post-test). *B*: effect of varying concentrations of receptor antagonists on spontaneously active DRG cultures at 14 DIV. Only the NK1 antagonist (L-732,138) and NK2 antagonist (GR-159,897) were able to fully inhibit spontaneous DRG activity (*$P < 0.05$, one-way ANOVA with Bonferroni post-test). *C*: effect of varying concentrations of receptor antagonists on bradykinin-induced DRG activity at 14 DIV. Retigabine and TTX are able to prevent both spontaneous and bradykinin-induced DRG activity, whereas the bradykinin B2 receptor antagonist WIN-64338 is only able to prevent bradykinin-induced DRG activity. *D*: the replacement of the cultures with fresh media (gray bars) results in a decrease in activity compared with control wells, where the media have not been replaced (black bars). Following treatment with 1 μM bradykinin (BK; hatched bars), DRG activity is increased compared with the untreated wells with fresh media, whereas 1 μM substance P (SP; checkered bars) has no effect. *E*: substance P ELISA showing no detectable levels of substance P in the media in the control condition and following application of either 1 μM bradykinin or capsaicin (CAP). Substance P was detected in the cell extract; however, this level remained unchanged following bradykinin or capsaicin treatment.

equipotent at both rat NK1 and NK2 receptors, with an IC_{50} of 0.3 and 0.4 μM, respectively (Cascieri et al. 1994; MacLeod et al. 1994). This, along with the potent nature of GR 159,897, indicates that NK2 receptors are potentially the predominant NK receptor subtype expressed in our DRG cultures. Along with NK receptors, functional bradykinin receptors are expressed within the cultures, as the addition of 1 μM bradykinin significantly increased DRG spontaneous activity (Fig. 6, *A* and *C*). However, addition of 10 μM WIN-64338, a bradykinin B2 receptor antagonist, did not significantly inhibit spontaneous DRG activity, indicating little, if any, endogenous bradykinin release in the DRG cultures. The augmentation in activity produced by bradykinin can be prevented by either the K_v activator retigabine or TTX (Fig. 6*C*), suggesting that bradykinin is unable to evoke activity once spontaneous firing has been significantly inhibited, regardless of mechanism. The lack of endogenous bradykinin in our culture was further demonstrated by showing that WIN-64338 was able to attenuate partially the bradykinin-induced increase in activity at 1 μM and fully inhibit the bradykinin-induced increase at 10 μM without affecting baseline spontaneous activity (Fig. 6*C*), as well as by replacing the culture media with fresh media and seeing a similar increase in spontaneous activity following the addition of 1 μM bradykinin (an approximate fourfold increase over control; Fig. 6*D*). As can also be seen in Fig. 6*D*, the replacement of the media with fresh media resulted in a significant decrease in spontaneous activity immediately following the replacement. Furthermore, both under control conditions (Fig. 6*A*) and following fresh media replacement (Fig. 6*D*), substance P did not evoke increases in spontaneous activity, suggesting that another unidentified tachykinin recep-

Table 3. *DRG receptor pharmacology*

Compound	Effect at 14 DIV
Glutamate	No effect $\leq$25 μM
NBQX	No effect $\leq$20 μM
NMDA	No effect $\leq$25 μM
APV	No effect $\leq$50 μM
GABA	No effect $\leq$100 μM
Picrotoxin	No effect $\leq$100 μM
Bradykinin	EC_{50} = 0.017 μM
WIN-64338	No effect $\leq$10 μM
Substance P	No effect $\leq$1 μM
L-732,138	IC_{50} = 1.5 μM
GR 159,897	IC_{50} = 0.18 μM

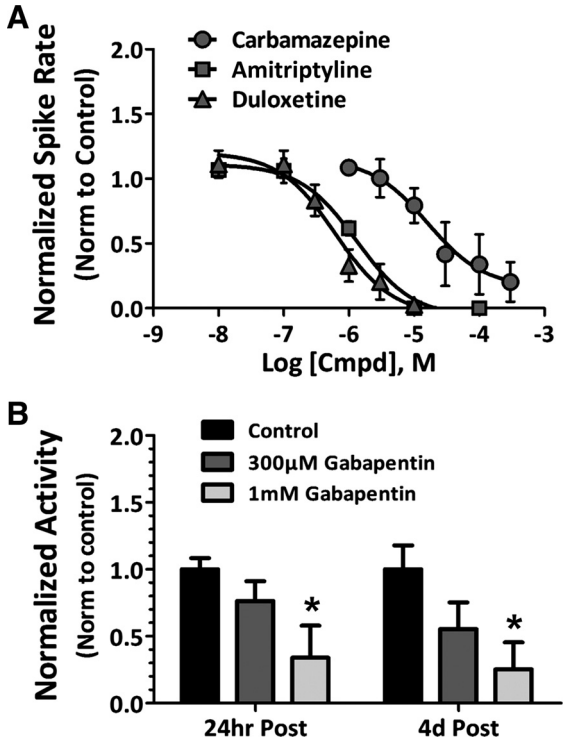

Fig. 7. Effect of clinically validated pain therapeutics on spontaneous DRG activity. *A*: concentration response curves for carbamazepine, amitriptyline, and duloxetine on spontaneously active DRG cultures at 14 DIV. IC_{50} values are given in Table 4. Cmpd, compound. *B*: effect of 300 μM (dark gray bars) and 1 mM (light gray bars) gabapentin at both 1 and 4 days post-treatment of spontaneously active DRG cultures on 14 DIV compared with control (black bars; $*P < 0.05$, two-way ANOVA with Bonferroni post-test).

tor ligand may be driving the NK2 receptor-dependent spontaneous activity. This was verified further through a substance P-specific ELISA assay, which showed no detectable levels of substance P in the media (Fig. 6*E*). There was, however, a relatively low level detected within the cell (~1 nM) that most likely represents a pool of unreleased substance P, since increasing DRG activity with either capsaicin or bradykinin did not lead to detectable levels of substance P in the media, whereas the intracellular levels remained unchanged (Fig. 6*E*).

To validate our spontaneously active rat DRG culture as a potential in vitro screening assay, we tested compounds from different drug classes commonly used in the treatment of neuropathic pain for their efficacy in reducing spontaneous firing rates. Figure 7*A* shows the concentration response curves for the anticonvulsant carbamazepine and two antidepressants—amitriptyline, a tricyclic antidepressant, and the serotonin-norepinephrine reuptake inhibitor duloxetine. All three compounds were able to reduce spontaneous DRG activity significantly, with duloxetine (IC_{50} = 0.62 μM) and amitriptyline (IC_{50} = 1.3 μM) exhibiting greater potency than carbamazepine (IC_{50} = 16.1 μM). Additionally, 1 mM of the Ca_V channel ligand gabapentin produced a significant reduction in DRG firing rates, beginning 24 h after treatment on 14 DIV (24 h: 66.0 ± 24.0% inhibition; 4 days: 74.8 ± 20.1% inhibition, n = 7; two-way ANOVA with Bonferroni post-test; Fig. 7*B*). At 300 μM, gabapentin produced modest inhibition of activity that was not statistically significant (24 h: 23.6 ± 14.7% inhibition; 4 days: 44.5 ± 19.7% inhibition, n = 15; two-way ANOVA with Bonferroni post-test; Fig. 7*B*). In contrast, morphine at 5 μM had no effect on DRG spontaneous activity, 1 h post-treatment (Table 4; data not shown). These data illustrate that these spontaneously active rat DRG cultures can be used to demonstrate the efficacy of select neuropathic pain drugs on reducing DRG hyperexcitability.

DISCUSSION

In this report, a functional in vitro rat DRG assay, using a multiwell MEA platform that records spontaneous activity from several DRG cells within multiple cultures simultaneously, is described. Optimal culture conditions, resulting in robust, spontaneous DRG firing to assess the ability of different compounds to augment or attenuate the activity recorded in our cultures, were determined. Pharmacological validation of this system was achieved by demonstrating that clinically effective anti-pain therapeutics produced the expected inhibition of electrical activity in the cultures. The development of this platform will allow for identification and characterization of potential pain therapeutics in a manner conducive to translational drug discovery.

Previous studies have shown that under typical culture conditions, adult rat DRG cells, isolated from noninjured animals, exhibit little or no spontaneous firing in vitro, unless they are treated chronically with NGF and incubated with more physiologic extracellular concentrations of NaCl (Kayano et al. 2013; Kitamura et al. 2005). We have extended these results to embryonic rat DRG cultures, a preparation more favorable to the large cell yields needed for multiwell MEA experiments. Since both spontaneous DRG activity and DRG NGF levels have been shown to be increased significantly in rat chronic pain models (Herzberg et al. 1997; Kajander et al. 1992), it has been suggested that chronic NGF-treated, hyperexcitable DRG cells could be used as an in vitro model of pain (Kitamura et al. 2005). Therefore, in these NGF-treated cultures, it was important to characterize the ion channels and receptors contributing to the underlying excitability to determine potential viable pain targets within this system. The results demonstrate that Na_V, K_v, and T-type Ca_V channels all play a role in modulating the spontaneous activity of our rat DRG cultures. Interestingly, there was little effect of high-threshold Ca_V channel blockers with our data, indicating that N- and R-type Ca_V channels do not contribute to spontaneous firing and that only a high concentration of the L-type Ca_V channel antagonist nifedipine was able to reduce activity. The inhibitory effects of 10 μM nifedipine could alternatively be due to activity at T-type Ca^{2+} channels, since nifedipine has been shown to inhibit T-type channels in the low micromolar range (Shcheglovitov et al. 2005). Furthermore, since high-threshold P/R-type Ca_V channels are typically involved in fast neurotransmitter release (e.g., glutamate), our results demonstrating the absence of both a glutamateric and a GABAergic drive within the DRG cul-

Table 4. *Clinically used compounds*

Compound	Effect at 14 DIV
Morphine	No effect ≦5 μM
Duloxetine	IC_{50} = 0.62 μM
Amitriptyline	IC_{50} = 1.3 μM
Gabapentin	Decreased spontaneous activity at 1 mM
Carbamazepine	IC_{50} = 16.2 μM

tures align with the limited participation of high-threshold Ca_V channel activity in spontaneous DRG firing. Additionally, the firing properties detailed in Table 1 indicate a predominantly asynchronous firing pattern with relatively few functional connections between cells, suggesting that the spontaneous DRG activity that we recorded was driven by high intrinsic excitability rather than synaptic activity.

In contrast, both neurokinin and bradykinin receptor ligands do appear to influence DRG excitability in our cultures. Whereas substance P specifically does not play a role in DRG activity in our cultures, antagonism of the NK2 receptor completely abolishes spontaneous DRG firing, suggesting that a different, as-yet unidentified NK ligand may be present in the extracellular medium. This conclusion is in contrast to a previous study showing that chronic NGF treatment increases substance P release in embyronic rat DRG cultures (Yang et al. 2007). Additionally, application of bradykinin produced a robust increase in DRG firing rates, whereas a bradykinin receptor antagonist had limited effects, indicating the presence of functional bradykinin receptors but little, if any, bradykinin present in the extracellular medium.

The proposal that this platform is translational as an in vitro pain model is supported by the ability of commonly used neuropathic pain therapeutics to suppress the spontaneous DRG activity recorded on the MEAs. The antiepileptic carbamazepine and the antidepressants duloxetine and amitriptyline all significantly reduced DRG firing. Carbamazepine stabilizes the inactivated state of Na_V (Rogawski and Loscher 2004) and has been shown to inhibit Na^+ currents in DRG cells (Rush and Elliott 1997). Duloxetine is a serotonin-norepinephrine-reuptake inhibitor and has been purported to be efficacious in neuropathic pain through this mechanism (Alba-Delgado et al. 2012). However, duloxetine has also been shown to be a potent inhibitor of Na_V (Wang et al. 2010), suggesting that this may be the mechanism by which it was able to suppress spontaneous DRG activity. Similarly, the tricyclic antidepressant amitriptyline, which also modulates biogenic amine neurotransmission, has also been shown to inhibit Na_V (Pancrazio et al. 1998). The hypothesis that these compounds are active in this assay due to effects on Na^+ channels, rather than biogenic amines, is further supported by the lack of effect of analgesics that are believed to work by reducing synaptic neurotransmitter release. Both the centrally acting compound morphine (Homma et al. 1983) and ziconotide, a synthetic form of the ω-conotoxin MVIIA toxin and selective inhibitor of N-type Ca_V channels (Bowersox et al. 1996), were not effective in reducing DRG firing. However, gabapentin, which has been purported to work through inhibiting high-threshold Ca_V channels (Hendrich et al. 2008; Sutton et al. 2002), was able to reduce spontaneous DRG activity significantly, albeit at a very high concentration (1 mM). This observed inhibitory effect of gabapentin on spontaneously firing DRG cells could alternatively be due to effects on membrane excitability, since gabapentin has been reported to reduce persistent Na^+ currents recorded from injured DRG neurons in vitro (Yang et al. 2009). Taken together, these data indicate that this platform may represent an effective in vitro pain model for predicting efficacy of compounds that target intrinsic excitability rather than neurotransmitter release from sensory neurons in the dorsal horn of the spinal cord. Future assay development using cocultures of DRG and dorsal horn spinal cord neurons may provide a path to evaluate the action of compounds on intrinsic excitability and neurotransmitter release within the central nervous system.

Whereas this assay does have the potential as a functional phenotypic screen for analgesics, it is worth pointing out several caveats. As mentioned, this assay, as is, would not identify novel compounds that work by modulating central synaptic transmission within the dorsal horn of the spinal cord. Furthermore, in this preparation, we have used embryonic rat DRG to increase throughput; however, the complement of ion channels and receptors in embryonic DRG does not fully recapitulate the expression profile found in adult DRG (Zhu and Oxford 2011). The predictive validity of this embryonic rat DRG MEA assay would therefore depend on the target of interest being expressed in both NGF-treated embryonic DRG and DRG from in vivo adult pain models. Finally, it is of note that whereas we have demonstrated efficacy in this assay with multiple therapeutics used to treat chronic pain, other compounds shown to reduce spontaneous rat DRG activity, such as NK1 antagonists, have shown limited clinical efficacy in humans. Whereas there is debate as to why preclinical data with NK1 antagonists have not been able to translate to the clinic (Hill 2000; Urban and Fox 2000), this does indicate that a spontaneously active rat DRG MEA assay may also be subjected to the same translational challenges seen in many other preclinical rodent pain models (Berge 2011; Percie du Sert and Rice 2014).

In summary, we have characterized an in vitro spontaneously active rat DRG assay using a multiwell MEA platform. We have demonstrated substantial and persistent spontaneous DRG activity that can be either suppressed or enhanced by targeting several different ion channels and receptors associated with generating or maintaining pain-like states. Finally, the throughput and phenotypic nature of this assay make it a useful in vitro model for evaluating the potential of many different mechanisms for the amelioration of chronic pain.

DISCLOSURES

All authors are employees of Bristol-Myers Squibb.

AUTHOR CONTRIBUTIONS

L.K. and J.D.G. conception and design of research; K.N., S.W., N.H., and J.D.G. performed experiments; K.N., S.W., N.H., J.H., and J.D.G. analyzed data; K.N., S.W., N.H., M.K.A., J.H., and J.D.G. interpreted results of experiments; J.D.G. prepared figures; K.N. and J.D.G. drafted manuscript; M.K.A., L.K., J.H., and J.D.G. edited and revised manuscript; K.N., S.W., N.H., M.K.A., L.K., J.H., and J.D.G. approved final version of manuscript.

REFERENCES

Abdulla FA, Smith PA. Nociceptin inhibits T-type Ca2+ channel current in rat sensory neurons by a G-protein-independent mechanism. *J Neurosci* 17: 8721–8728, 1997.

Alba-Delgado C, Mico JA, Sanchez-Blazquez P, Berrocoso E. Analgesic antidepressants promote the responsiveness of locus coeruleus neurons to noxious stimulation: implications for neuropathic pain. *Pain* 153: 1438–1449, 2012.

Berge OG. Predictive validity of behavioural animal models for chronic pain. *Br J Pharmacol* 164: 1195–1206, 2011.

Bezprozvanny I, Tsien RW. Voltage-dependent blockade of diverse types of voltage-gated Ca2+ channels expressed in *Xenopus oocytes* by the Ca2+ channel antagonist mibefradil (Ro 40-5967). *Mol Pharmacol* 48: 540–549, 1995.

Bowersox SS, Gadbois T, Singh T, Pettus M, Wang YX, Luther RR. Selective N-type neuronal voltage-sensitive calcium channel blocker, SNX-111, produces spinal antinociception in rat models of acute, persistent and neuropathic pain. *J Pharmacol Exp Ther* 279: 1243–1249, 1996.

Cascieri MA, Macleod AM, Underwood D, Shiao LL, Ber E, Sadowski S, Yu H, Merchant KJ, Swain CJ, Strader CD, Fong TM. Characterization of the interaction of *N*-acyl-L-tryptophan benzyl ester neurokinin antagonists with the human neurokinin-1 receptor. *J Biol Chem* 269: 6587–6591, 1994.

Chiappalone M, Vato A, Berdondini L, Koudelka-Hep M, Martinoia S. Network dynamics and synchronous activity in cultured cortical neurons. *Int J Neural Syst* 17: 87–103, 2007.

Clozel JP, Ertel EA, Ertel SI. Discovery and main pharmacological properties of mibefradil (Ro 40-5967), the first selective T-type calcium channel blocker. *J Hypertens Suppl* 15: S17–S25, 1997.

Djouhri L, Al Otaibi M, Kahlat K, Smith T, Sathish J, Weng X. Persistent hindlimb inflammation induces changes in activation properties of hyperpolarization-activated current (Ih) in rat C-fiber nociceptors in vivo. *Neuroscience* 301: 121–133, 2015.

Djouhri L, Koutsikou S, Fang X, McMullan S, Lawson SN. Spontaneous pain, both neuropathic and inflammatory, is related to frequency of spontaneous firing in intact C-fiber nociceptors. *J Neurosci* 26: 1281–1292, 2006.

Everill B, Kocsis JD. Nerve growth factor maintains potassium conductance after nerve injury in adult cutaneous afferent dorsal root ganglion neurons. *Neuroscience* 100: 417–422, 2000.

Gourevitch B, Eggermont JJ. A nonparametric approach for detection of bursts in spike trains. *J Neurosci Methods* 160: 349–358, 2007.

Hama A, Sagen J. Antinociceptive effects of the marine snail peptides conantokin-G and conotoxin MVIIA alone and in combination in rat models of pain. *Neuropharmacology* 56: 556–563, 2009.

Heinke B, Balzer E, Sandkuhler J. Pre- and postsynaptic contributions of voltage-dependent Ca2+ channels to nociceptive transmission in rat spinal lamina I neurons. *Eur J Neurosci* 19: 103–111, 2004.

Hendrich J, Van Minh AT, Heblich F, Nieto-Rostro M, Watschinger K, Striessnig J, Wratten J, Davies A, Dolphin AC. Pharmacological disruption of calcium channel trafficking by the alpha2delta ligand gabapentin. *Proc Natl Acad Sci USA* 105: 3628–3633, 2008.

Herzberg U, Eliav E, Dorsey JM, Gracely RH, Kopin IJ. NGF involvement in pain induced by chronic constriction injury of the rat sciatic nerve. *Neuroreport* 8: 1613–1618, 1997.

Hill R. NK1 (substance P) receptor antagonists—why are they not analgesic in humans? *Trends Pharmacol Sci* 21: 244–246, 2000.

Homma E, Collins JG, Kitahata LM, Matsumoto M, Kawahara M. Suppression of noxiously evoked WDR dorsal horn neuronal activity by spinally administered morphine. *Anesthesiology* 58: 232–236, 1983.

Huguenard JR. Low-threshold calcium currents in central nervous system neurons. *Annu Rev Physiol* 58: 329–348, 1996.

Jarvis MF, Honore P, Shieh CC, Chapman M, Joshi S, Zhang XF, Kort M, Carroll W, Marron B, Atkinson R, Thomas J, Liu D, Krambis M, Liu Y, McGaraughty S, Chu K, Roeloffs R, Zhong C, Mikusa JP, Hernandez G, Gauvin D, Wade C, Zhu C, Pai M, Scanio M, Shi L, Drizin I, Gregg R, Matulenko M, Hakeem A, Gross M, Johnson M, Marsh K, Wagoner PK, Sullivan JP, Faltynek CR, Krafte DS. A-803467, a potent and selective Nav1.8 sodium channel blocker, attenuates neuropathic and inflammatory pain in the rat. *Proc Natl Acad Sci USA* 104: 8520–8525, 2007.

Jevtovic-Todorovic V, Todorovic SM. The role of peripheral T-type calcium channels in pain transmission. *Cell Calcium* 40: 197–203, 2006.

Kajander KC, Wakisaka S, Bennett GJ. Spontaneous discharge originates in the dorsal root ganglion at the onset of a painful peripheral neuropathy in the rat. *Neurosci Lett* 138: 225–228, 1992.

Kayano T, Kitamura N, Moriya T, Kuwahara T, Komagiri Y, Toescu EC, Shibuya I. Chronic NGF treatment induces somatic hyperexcitability in cultured dorsal root ganglion neurons of the rat. *Biomed Res* 34: 329–342, 2013.

Kitamura N, Konno A, Kuwahara T, Komagiri Y. Nerve growth factor-induced hyperexcitability of rat sensory neuron in culture. *Biomed Res* 26: 123–130, 2005.

Lee JH, Gomora JC, Cribbs LL, Perez-Reyes E. Nickel block of three cloned T-type calcium channels: low concentrations selectively block alpha1H. *Biophys J* 77: 3034–3042, 1999.

Liu R, Lin G, Xu H. An efficient method for dorsal root ganglia neurons purification with a one-time anti-mitotic reagent treatment. *PLoS One* 8: e60558, 2013.

Ma C, LaMotte RH. Multiple sites for generation of ectopic spontaneous activity in neurons of the chronically compressed dorsal root ganglion. *J Neurosci* 27: 14059–14068, 2007.

MacLeod AM, Merchant KJ, Brookfield F, Kelleher F, Stevenson G, Owens AP, Swain CJ, Casiceri MA, Sadowski S, Ber E, Strader CD, MacIntyre DE, Metzger JM, Ball RG, Baker R. Identification of L-tryptophan derivatives with potent and selective antagonist activity at the NK1 receptor. *J Med Chem* 37: 1269–1274, 1994.

Massobrio P, Tessadori J, Chiappalone M, Ghirardi M. In vitro studies of neuronal networks and synaptic plasticity in invertebrates and in mammals using multielectrode arrays. *Neural Plast* 2015: 196195, 2015.

McConnell ER, McClain MA, Ross J, Lefew WR, Shafer TJ. Evaluation of multi-well microelectrode arrays for neurotoxicity screening using a chemical training set. *Neurotoxicology* 33: 1048–1057, 2012.

Mishra SK, Hermsmeyer K. Selective inhibition of T-type Ca2+ channels by Ro 40-5967. *Circ Res* 75: 144–148, 1994.

Newcomb R, Szoke B, Palma A, Wang G, Chen X, Hopkins W, Cong R, Miller J, Urge L, Tarczy-Hornoch K, Loo JA, Dooley DJ, Nadasdi L, Tsien RW, Lemos J, Miljanich G. Selective peptide antagonist of the class E calcium channel from the venom of the tarantula Hysterocrates gigas. *Biochemistry* 37: 15353–15362, 1998.

Pancrazio JJ, Kamatchi GL, Roscoe AK, Lynch C 3rd. Inhibition of neuronal Na+ channels by antidepressant drugs. *J Pharmacol Exp Ther* 284: 208–214, 1998.

Passmore GM, Selyanko AA, Mistry M, Al-Qatari M, Marsh SJ, Matthews EA, Dickenson AH, Brown TA, Burbidge SA, Main M, Brown DA. KCNQ/M currents in sensory neurons: significance for pain therapy. *J Neurosci* 23: 7227–7236, 2003.

Percie du Sert N, Rice AS. Improving the translation of analgesic drugs to the clinic: animal models of neuropathic pain. *Br J Pharmacol* 171: 2951–2963, 2014.

Perney MT, Hirning LD, Leeman SE, Miller RJ. Multiple calcium channels mediate neurotransmitter release from peripheral neurons. *Proc Natl Acad Sci USA* 83: 6656–6659, 1986.

Rogawski MA, Loscher W. The neurobiology of antiepileptic drugs. *Nat Rev Neurosci* 5: 553–564, 2004.

Rush AM, Elliott JR. Phenytoin and carbamazepine: differential inhibition of sodium currents in small cells from adult rat dorsal root ganglia. *Neurosci Lett* 226: 95–98, 1997.

Schmalhofer WA, Calhoun J, Burrows R, Bailey T, Kohler MG, Weinglass AB, Kaczorowski GJ, Garcia ML, Koltzenburg M, Priest BT. ProTx-II, a selective inhibitor of NaV1.7 sodium channels, blocks action potential propagation in nociceptors. *Mol Pharmacol* 74: 1476–1484, 2008.

Shcheglovitov A, Zhelay T, Vitko Y, Osipenko V, Perez-Reyes E, Kostyuk P, Shuba Y. Contrasting the effects of nifedipine on subtypes of endogenous and recombinant T-type Ca2+ channels. *Biochem Pharmacol* 69: 841–854, 2005.

Study RE, Kral MG. Spontaneous action potential activity in isolated dorsal root ganglion neurons from rats with a painful neuropathy. *Pain* 65: 235–242, 1996.

Sutton KG, Martin DJ, Pinnock RD, Lee K, Scott RH. Gabapentin inhibits high-threshold calcium channel currents in cultured rat dorsal root ganglion neurones. *Br J Pharmacol* 135: 257–265, 2002.

Todorovic SM, Jevtovic-Todorovic V. The role of T-type calcium channels in peripheral and central pain processing. *CNS Neurol Disord Drug Targets* 5: 639–653, 2006.

Todorovic SM, Lingle CJ. Pharmacological properties of T-type Ca2+ current in adult rat sensory neurons: effects of anticonvulsant and anesthetic agents. *J Neurophysiol* 79: 240–252, 1998.

Urban LA, Fox AJ. NK1 receptor antagonists—are they really without effect in the pain clinic? *Trends Pharmacol Sci* 21: 462–464; author reply 465, 2000.

Wainger BJ, Buttermore ED, Oliveira JT, Mellin C, Lee S, Saber WA, Wang AJ, Ichida JK, Chiu IM, Barrett L, Huebner EA, Bilgin C, Tsujimoto N, Brenneis C, Kapur K, Rubin LL, Eggan K, Woolf CJ. Modeling pain in vitro using nociceptor neurons reprogrammed from fibroblasts. *Nat Neurosci* 18: 17–24, 2015.

Wang SY, Calderon J, Kuo Wang G. Block of neuronal Na+ channels by antidepressant duloxetine in a state-dependent manner. *Anesthesiology* 113: 655–665, 2010.

Weng X, Smith T, Sathish J, Djouhri L. Chronic inflammatory pain is associated with increased excitability and hyperpolarization-activated current (Ih) in C- but not Adelta-nociceptors. *Pain* 153: 900–914, 2012.

Xie W, Strong JA, Meij JT, Zhang JM, Yu L. Neuropathic pain: early spontaneous afferent activity is the trigger. *Pain* 116: 243–256, 2005.

Xie W, Strong JA, Zhang JM. Increased excitability and spontaneous activity of rat sensory neurons following in vitro stimulation of sympathetic fiber sprouts in the isolated dorsal root ganglion. *Pain* 151: 447–459, 2010.

Yang RH, Wang WT, Chen JY, Xie RG, Hu SJ. Gabapentin selectively reduces persistent sodium current in injured type-A dorsal root ganglion neurons. *Pain* 143: 48–55, 2009.

Yang XD, Liu Z, Liu HX, Wang LH, Ma CH, Li ZZ. Regulatory effect of nerve growth factor on release of substance P in cultured dorsal root ganglion neurons of rat. *Neurosci Bull* 23: 215–220, 2007.

Zamponi GW, Lewis RJ, Todorovic SM, Arneric SP, Snutch TP. Role of voltage-gated calcium channels in ascending pain pathways. *Brain Res Rev* 60: 84–89, 2009.

Zhu W, Galoyan SM, Petruska JC, Oxford GS, Mendell LM. A developmental switch in acute sensitization of small dorsal root ganglion (DRG) neurons to capsaicin or noxious heating by NGF. *J Neurophysiol* 92: 3148–3152, 2004.

Zhu W, Oxford GS. Differential gene expression of neonatal and adult DRG neurons correlates with the differential sensitization of TRPV1 responses to nerve growth factor. *Neurosci Lett* 500: 192–196, 2011.